

Microscopic Deformation of Filler Particles in Rubber Under Uniaxial Deformation

Gábor Belina,^{*1} Volker Urban,¹ Ekkehard Straube,² Wim Pyckhout-Hintzen,³ Manfred Klüppel,⁴ Gert Heinrich⁵

¹ European Synchrotron Radiation Facility, B.P. 220, 38043 Grenoble, France

² Martin-Luther-University Halle-Wittenberg, D-06099 Halle (Saale), Germany

³ Forschungszentrum Jülich, D-52425 Jülich, Germany

⁴ DIK “German Institute for Rubber Technology”, D-30519 Hannover, Germany

⁵ Continental AG, D-30419 Hannover, Germany

Email: belina@esrf.fr

Summary: Structural studies of filled polymer networks under periodic deformation are of great importance to the industries concerned with rubber. The degree of reinforcement provided by the filler depends on a number of variables: the size of the polymer-filler interface, the size of primary particles, the size and shape of filler clusters. In the tyre industry it is necessary to optimize mechanical properties such as low rolling resistance, good wet grip and long lifetime. There have been studies of unfilled polymer networks and filler model-systems (block copolymers),^[1,2] but because their complexity, industrial rubber samples have escaped investigations. We performed SAXS, USAXS and SANS measurements on carbon black filled natural rubber (poly-isoprene) under uniaxial deformation at ESRF ID-02 and Forschungszentrum Jülich KWS-2. The scattering patterns of the studied filler particles show power-law decay over many decades in scattering vector q . At the scale of primary particles we detected surface fractal behavior and for the characteristic size of the primary particles we calculated lengths of the order of 10 nm. X-ray scattering was used for time resolved experiments (about 10 frames per second) and neutron scattering was used to distinguish between scattering from the studied fillers and the additives (especially zinc oxide) used in industrial materials.

Keywords: carbon black; neutron scattering; rubber; SAXS; uniaxial

Introduction

It is well known that particulate fillers such as carbon black increase the strength of vulcanized rubber more than tenfold, so it is hardly surprising that very few applications of elastomers use the polymer in the unfilled state. The fillers increase the tear strength, tensile strength, abrasion resistance and the modulus of elasticity of the elastomers. The most commonly used reinforcing

fillers are carbon blacks and silicas. Carbon blacks are a representative example for reinforcing fillers because of tonnage and their variety of properties. Carbon blacks for reinforcing purposes are manufactured by incomplete combustion of hydrocarbons (furnace blacks) or by thermal cracking (thermal blacks).

The degree of reinforcement provided by a filler depends on a number of variables: the specific surface area, interaction with the rubber matrix, the formation of filler clusters and their orientation. The primary particles during the manufacturing process of reinforcing fillers form aggregates, which, during incorporation into the rubber matrix, may form agglomerates and, if in sufficient concentration, a percolation network.

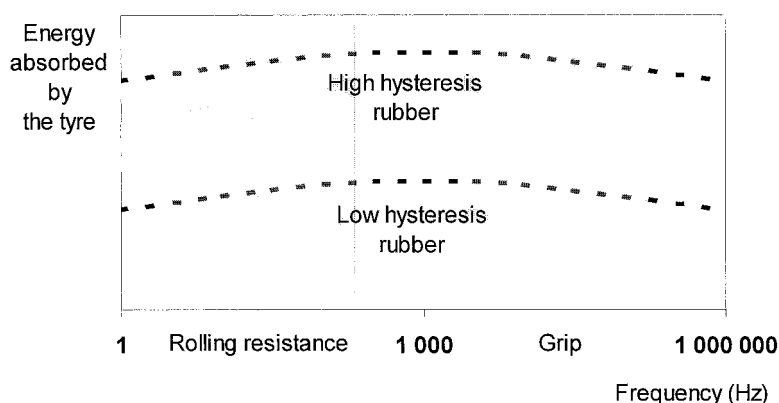


Fig. 1. Energy absorbed by the tyre during rolling and braking.^[4]

The biggest industrial use of carbon black filled rubber is the tyre industry, and regardless of their application all tyres must fulfill a fundamental set of functions: provide load-carrying capacity, cushioning and dampening, cornering force, dimensional stability, minimum noise and minimum vibration, transmit driving and braking torque, resist abrasion, generate steering response, have low rolling resistance and be durable throughout the expected life span.^[3] If a rubber compound has high hysteresis during periodical deformation it absorbs more energy, which is essential in road holding, especially during braking. On the other hand it is less

economic because it consumes more fuel during rolling. The contrary is true for the low hysteresis rubber compound (Figure 1). As the energy absorbed largely depends on the structure of the reinforcing filler clusters, it is important to understand the structural changes during deformation.

To study the structure of carbon black filled samples one cannot use many of the conventional measuring techniques such as optical microscopy and light scattering because carbon black absorbs most visible light. The use of electron microscopy leads to difficulties in interpreting these micrographs because of the superposition of 3D structures. SAXS and SANS are ideal for studying these materials because they can probe 3D space.

Experimental

The reinforcing filler in the studied rubber compound is a hard grade carbon black for rubber; its ASTM (American Standard of Testing Materials) number is N339. Its application is in the tyre treads, because this filler gives very good abrasion resistance to the rubber. The elastomer matrix is natural rubber.

The experiments were carried out at ESRF ID02^[5-7] and Forschungszentrum Jülich KWS-1.^[8] The experimental setup is shown schematically in Figure 2.

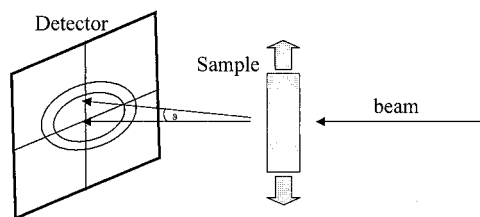


Fig. 2. Setup for SAXS and SANS experiments.

The scattered intensity is recorded (in function of scattering angle θ) on a 2D detector. The scattering vector is calculated as shown in equation (1)

$$q(\theta) = \frac{4\pi}{\lambda} \sin \frac{\theta}{2} \quad (1)$$

Where λ is the wavelength of the incident beam. The use of synchrotron X-ray radiation is very effective due to its high flux; it can be used to probe fast changes in microscopic structure.

However, industrial rubber contains many additives beside the reinforcing filler, among which is ZnO. The electron density of Zn is very high compared to that of carbon and complementary measurements are needed to distinguish the scattering signal of the filler from background intensities of other additives. Small Angle Neutron Scattering is a perfect tool for this task, since for neutrons the scattering length density of Zn and carbon is similar and the concentration difference is so huge that the scattering contribution of Zn is negligible.

Results and Discussion

We used the unified fit approach developed by Beaucage,^[9-10] which can describe materials showing microstructural features on many length scales. The unified equation describes material microstructure in terms of levels of structure. Each level of structure corresponds to a Guinier regime combined with a structurally limited power-law regime.^[10] The power-law serves to describe the properties of the structure, while the Guinier regime describes the size. The unified equation for a single structural level is given by equation (2).

$$I(q) = G \exp\left(-\frac{q^2 R_g^2}{3}\right) + B \left\{ \frac{\left[\operatorname{erf}\left(\frac{q R_g}{\sqrt{6}}\right) \right]^3}{q} \right\}^p \quad (2)$$

Where R_g is the radius of gyration, B is a constant prefactor, p : power law exponent. G is the Guinier prefactor shown in equation (3)

$$G = n^2 N_p I_e \quad (3)$$

n is the number of electrons in a particle, N_p is the number of particles in the scattering volume and I_e is the scattering factor for a single electron. For an arbitrary number of interrelated structural levels:

$$I(q) \cong \sum_{i=1}^n \left(G_i \exp\left(-\frac{q^2 R_{g_i}^2}{3}\right) + B_i \exp\left(-\frac{q^2 R_{g(i-1)}^2}{3}\right) \left\{ \frac{\left[\operatorname{erf}\left(\frac{q R_{g_i}}{\sqrt{6}}\right) \right]^3}{q} \right\}^{p_i} \right) \quad (4)$$

Eq. 4 can be simplified by introducing q_{limited} , which serves to limit the power law regime at low q . Thus

$$I(q) \cong \sum_{i=1}^n \left(G_i \exp \left(-\frac{q^2 R_{g_i}^2}{3} \right) + B_i \exp \left(-\frac{q^2 R_{g_{(i-1)}}^2}{3} \right) \left(\frac{1}{q_{i,\text{limited}}} \right)^{p_i} \right); \quad (5)$$

$$q_{\text{limited}} = \frac{q}{\left[\text{erf} \left(\frac{q R_{g_i}}{\sqrt{6}} \right) \right]^3}$$

Where $i=1$ stands for the smallest structural level. From the power law exponent the corresponding fractal dimension can be derived, which, for the case of carbon blacks at larger q range, is d_s , the surface fractal dimension,^[10-12] where $p = (6-d_s)$. For smaller q it becomes a mass fractal ($p = -d_m$). Figure (3) shows a scattering curve and how the unified equation describes the different structural levels. The two components of scattering for a single structural level are easily distinguished in a $\log(I)$ vs. $\log(q)$ plot, the power law appearing as a straight

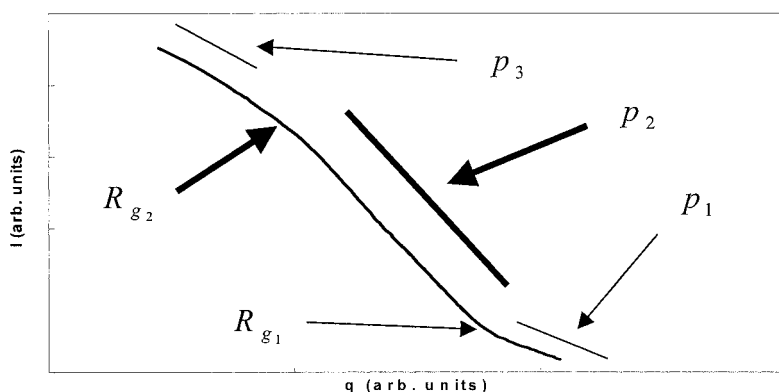


Fig. 3. Scattering curve from imaginary objects, showing microstructural features over several length scales. The thick arrows stand for one length scale.

line and the Guinier regime as a shoulder. One can imagine an aggregate with some kind of fractal structure that is described by its fractal dimension represented as a power law P_3 in the scattering curve. At the next level of smaller length scale, such an aggregate is composed of primary particles with a radius of gyration R_{g2} , and a surface fractal structure of the primary

particle represented by the power law P_2 . Finally, primary particles are made up of smaller building blocks of size R_{g1} and inner structure P_1 .

Figure (4) presents the scattering curves from neutron and x-ray experiments and how the unified fit is applied.

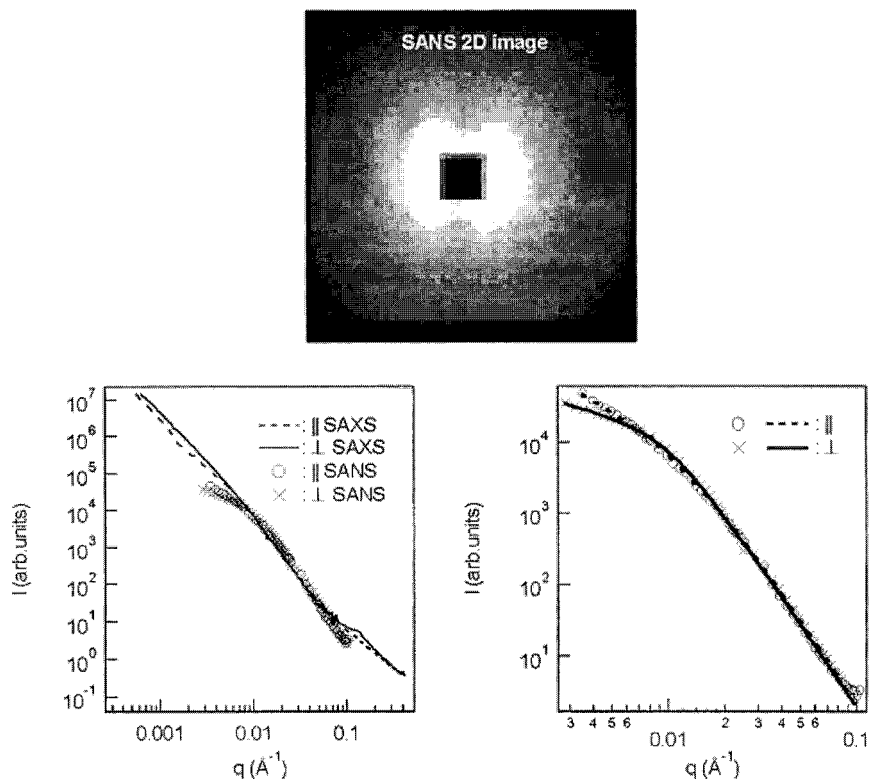


Fig. 4. Two-dimensional image of SANS and scattering curves from SAXS and SANS. The solid lines and the x markers stand for the perpendicular direction, the dashed lines and open circles for the parallel. On the left graph the markers are SANS; lines are SAXS data sets, stretch ratio: $\lambda = 2.5$; carbon black filler concentration is 40 w/w% ($\phi = 0.22$ v/v). On the right graph lines are fits from the unified approach and symbols are SANS data sets of the same sample. The power law exponents for the low q part of the curves: $p_{\parallel} = -1.8$; $p_{\perp} = -1$; for the high q part: $p_{\parallel} = p_{\perp} = -3.8$; radius of gyration: $R_{g\parallel} = 181 \text{\AA}$; $R_{g\perp} = 187 \text{\AA}$.

Among the additives of the industrial rubber there is ZnO_2 which gives a very strong signal in X-ray measurements, the scattering contribution of Zn is one order of magnitude stronger than

that of the carbon. The scattering length density of Zn is similar to that of the filler and because of the small volume fraction of ZnO_2 , it gives a negligible scattering contribution in SANS. In this way we are able to subtract the background that is produced by the matrix and the additives from the experimental measurements. The difference between the scattering length densities of the polymer matrix and the filler particles is much larger than the differences we get with X-rays. With SANS measurements we are able to look only at the filler without the surrounding material. From the SANS experiments it is clear that the scattering curves represent the carbon black filler even at low q , while for X-rays this is not true. The difference of the parallel and perpendicular direction comes from the difference in interparticle distances but not of the CB but of the ZnO .

For neutrons the difference is due to the structural changes in CB aggregates. The power law exponent at the carbon black primary particle level ($0.01 < q < 0.05$) is close to -3.8 for all of the samples. This can be explained by surface fractal model based on fairly rough particles, with surface fractal scaling extending over almost a decade in size. The final part of the SANS scattering curve is the beginning of the power law regime for the next structural level, which in this case is the aggregate. Care must be taken when analysing the power law exponents from these parts of the scattering curves because they do not extend over a very large q range.

On the images of the stretched samples we detected orientations of the filler particles, similar to those of SAXS, but we are able to say with more certainty that they are only the result of the deformation of the carbon black filler network and not of the additives containing heavy elements. On the two dimensional images we saw "butterfly" patterns, which are usually attributed to inhomogeneous deformation in the range of the length scale corresponding to the scattering vector at the highest intensity of the pattern. The length scale of the deformation calculated from the scattering curves starts at approximately 20 nm, which corresponds to the CB aggregate level.

Conclusion

We studied the deformation dependence of the filler particles in rubber and used the unified equation to interpret the experimental data. We performed both SAXS and SANS experiments. The reason for using X-rays is the possibility of making the fast measurements needed to study

the properties of the samples in conditions similar to those during operation. However from the comparison of the SAXS and SANS experiments we concluded that the addition of ZnO in industrial samples prevents the use of X-rays, the scattering contribution of Zn being too large compared to that of the carbon. The use of neutron scattering on samples containing heavy elements in small quantities still allows one to subtract the background from the scattering of the filler with reasonable certainty.

Acknowledgement

We thank the European Community in their program "Jülich Neutrons for Europe" for their financial support and ESRF for provision of beamtime and financial support.

- [1] E. Straube, V. Urban, W. Pyckhout-Hintzen, D. Richter, C. J. Glinka, *Phys. Rev. Lett.* **1995**, 74, 4464.
- [2] S. Westermann, M. Kreitschmann, W. Pyckhout-Hintzen, D. Richter, E. Straube, *Physica B* **1997**, 234-236, 306.
- [3] W. W. Barbin, M. B. Rodgers in: "*Science and Technology of Rubber*", 2nd ed., J. E. Mark, B. Erman, F. R. Eirich, Eds., Academic Press, 1994.
- [4] http://www.michelin.com/corporate/en/innovation/archives_tires_low.jsp
- [5] P. Bösecke, *Rev. Sci. Instrum.* **1992**, 63, 438.
- [6] P. Bösecke, O. Diat, *J. Appl. Crystallogr.* **1997**, 30, 867.
- [7] T. Narayanan, O. Diat, P. Bösecke, *Nucl. Instr. and Meth. in Phys. Res. A* **2001**, 467-468, 1005.
- [8] http://www.fz-juelich.de/iff/Institute/ins/Broschuere_NSE/kws2.shtml
- [9] G. Beaucage, *J. Appl. Cryst.* **1995**, 28, 717.
- [10] G. Beaucage, S. Rane, D. W. Schaefer, G. Long, D. Fischer, *J. Polym. Sci. Part B* **1999**, 37, 1105.
- [11] F. Ehrburger-Dolle, M. Hindermann-Bischoff, F. Livet, F. Bley, C. Rochas, E. Geissler, *Langmuir* **2001**, 17, 329.
- [12] T. P. Rieker, M. Hindermann-Bischoff, F. Ehrburger-Dolle, *Langmuir* **2000**, 16, 5588-5592.